AD-A083 968 CHARLES STARK DRAPER LAB INC CAMBRIDGE MA F/G 17/7
MATERIALS RESEARCH FOR ADVANCED INERTIAL INSTRUMENTATION. TASK --ETC(U)
OCT 79 D DAS, K KUMAR, E WETTSTEIN N00014-77-C-0388
UNCLASSIFIED R-1306 NL

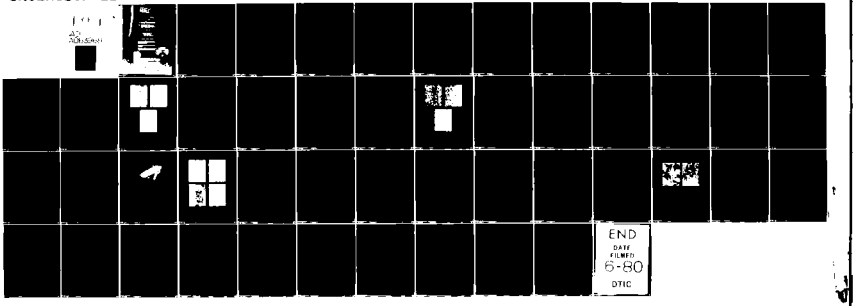

(9) Technical report no. 2, 1 Jul '78 30 Sep '79

UNCLASSIFIED

SECURITY CLASSIFICATION OF THIS PAGE (When Data Entered)

REPORT DOCUMENTATION PAGE

READ INSTRUCTIONS BEFORE COMPLETING FORM

1. REPORT NUMBER: Technical Report No. 2
2. GOVT ACCESSION NO.: AD-A083968
3. RECIPIENT'S CATALOG NUMBER:

4. TITLE (and Subtitle): (6) Materials Research for Advanced Inertial Instrumentation, Task 3. Rare Earth Magnetic Material Technology as Related to Gyro Torquers and Motors.

5. TYPE OF REPORT & PERIOD COVERED: Research Report 7/1/78 - 9/30/79

6. PERFORMING ORG. REPORT NUMBER: (8) R-1306

7. AUTHOR(s): (10) D. Das, K. Kumar and E. Wettstein

8. CONTRACT OR GRANT NUMBER(s): (15) N00014-77-C-0388

9. PERFORMING ORGANIZATION NAME AND ADDRESS:
The Charles Stark Draper Laboratory, Inc.
555 Technology Square
Cambridge, Massachusetts 02139

10. PROGRAM ELEMENT, PROJECT, TASK AREA & WORK UNIT NUMBERS: (12) 59

11. CONTROLLING OFFICE NAME AND ADDRESS:
Office of Naval Research
Department of the Navy
800 N. Quincy Street, Arlington, Virginia 20217

12. REPORT DATE: (11) Oct[illegible]79

13. NUMBER OF PAGES: 36

14. MONITORING AGENCY NAME & ADDRESS (if different from Controlling Office):
Office of Naval Research
Boston Branch, Bldg. 114, Sec.D
666 Summer Street
Boston, MA 02210

15. SECURITY CLASS. (of this report): Unclassified

15a. DECLASSIFICATION/DOWNGRADING SCHEDULE:

16. DISTRIBUTION STATEMENT (of this Report):

Approved for public release, distribution unlimited

17. DISTRIBUTION STATEMENT (of the abstract entered in Block 20, if different from Report):

18. SUPPLEMENTARY NOTES:

19. KEY WORDS (Continue on reverse side if necessary and identify by block number):

Cobalt
Coercivity
Hot Isostatic Pressing
Magnet
Samarium
Stability
Temperature Compensation

20. ABSTRACT (Continue on reverse side if necessary and identify by block number):

For inertial applications, high-energy-product $SmCo_5$ magnets are required which possess very low flux decay rate, near zero temperature coefficient of magnetization, and thermal expansion coefficient similar to that of beryllium. Concentrated effort has been directed towards achieving and understanding the underlying mechanism of high flux stability. In the ensuing period, efforts will be directed towards temperature compensation and tailoring of thermal expansion along with further studies on stability.
(Continued on reverse side)

DD FORM 1 JAN 73 1473 EDITION OF 1 NOV 65 IS OBSOLETE

UNCLASSIFIED

SECURITY CLASSIFICATION OF THIS PAGE (When Data Entered)

408386

JOB

By controlling the maximum level of oxygen content to about 0.6 weight percent, along with fine grain size in the final sintered product, we have been able to produce some outstanding magnetic properties, such as $(BH)_{max}$ ~20 mGOe, H_{ci} ~50 kOe, and H_k of 33.5 kOe. This has resulted in a low flux decay rate of 700 ppm/decade of days. This translates into a decay rate of less than a ppm/day in the third decade of time which is the decade of interest. With special stabilizing treatments, which are planned, the stability value may be reduced further, perhaps by as much as an order of magnitude.

Our arc-plasma-sprayed magnets with an oxygen content of about 0.15 percent possess a low decay rate of 50 ppm/decade. Unfortunately, their energy products are low because of the random grain orientation. Our immediate goal is to produce aligned and densified powder metallurgical magnets with oxygen content of APS magnets. To accomplish that, we have already developed a hot isostatic pressing process in this program, which gives us nearly 100 percent dense magnets of fine and aligned grain structure with little if any oxygen pickup above that of the starting powder compact. Our exploratory research in the latter area has produced extremely promising results for production of powder and compaction with an oxygen level no higher than in our APS magnets. We, therefore, have the basic results and processes to feel very optimistic about our prospects of achieving our extremely difficult goals in this area.

R-1306

MATERIALS RESEARCH FOR ADVANCED INERTIAL INSTRUMENTATION

TASK 3: RARE EARTH MAGNETIC MATERIAL TECHNOLOGY AS RELATED TO GYRO TORQUERS AND MOTORS

October 1979

TECHNICAL REPORT No. 2
FOR THE PERIOD
July 1, 1978 to September 30, 1979

by

D. Das
K. Kumar
E. Wettstein

Prepared for the Office of Naval Research
Department of the Navy, under Contract N00014-77-C-0388

Approved: M.S. Sapuppo

M.S. Sapuppo, Head
Component Development
Department

The Charles Stark Draper Laboratory, Inc.
Cambridge, Massachusetts 02139

ACKNOWLEDGEMENT

We wish to express our appreciation to the National Magnet Laboratory, MIT, for their assistance by making their high-field magnets available for our studies in this program. Our sincere thanks to C.R. Dauwalter for carrying out the flux stability measurements.

This report was prepared by The Charles Stark Draper Laboratory, Inc., under Contract N00014-77-C-0388 with the Office of Naval Research of the Department of the Navy, with Dr. F.S. Gardner of ONR, Boston, serving as Scientific Officer.

Publication of this report does not constitute approval by the U.S. Navy of the findings or conclusions contained herein. It is published for the exchange and stimulation of ideas.

TABLE OF CONTENTS

LIST OF FIGURES

LIST OF TABLES

SECTION 1

INTRODUCTION

1.1 Program Background

The Charles Stark Draper Laboratory, Inc. (CSDL) is involved in research and development over a broad spectrum of technology associated with guidance, navigation, and control for vehicles of all types. One of the areas of importance to advancements in inertial navigation systems is the improvement of magnetic devices serving critical functions in these systems. Samarium-cobalt magnet devices are used within inertial systems as components of the inertial instruments or sensors—the gyro and accelerometer—and as gimbal torque motors. As an example of the former category, samarium-cobalt permanent magnets are employed in the torque generator, or angular motion forcer, of the movable and buoyant member of the instrument. The torque generator is of cylindrical geometry, and in many designs the magnets are located on the moving member which must remain buoyant in fluid. Here the lower volume of the magnet derived from the high energy product of $SmCo_5$ magnets impacts favorably on the overall size and weight of the completed instrument.

Rare-earth cobalt magnets, because of their large maximum energy product, $(BH)_{max}$, are ideally suited for many other applications requiring high magnetic strength. Because of the large $(BH)_{max}$ a lesser volume of magnet is required to produce a given amount of magnetic flux in a device.

In addition to high energy product, magnets utilized in precision inertial instruments must also possess excellent long-term flux

stability, insensitivity to temperature change, and physical properties compatible with beryllium. Because of its favorable strength-to-weight ratio, beryllium is the structural material of choice in modern inertial instruments.

A comprehensive program to develop samarium-cobalt magnets by powder-metallurgy techniques for applications as components in new and future generations of inertial instruments was initiated at the Draper Laboratory in October 1977 under the sponsorship of the Office of Naval Research. The objectives of the program were to develop improved sintering procedures to fabricate inertial-grade $SmCo_5$ magnets with improvements in three areas mentioned above: long-term flux stability, reduced temperature coefficient, and tailoring of the thermal expansion coefficient to match that of beryllium.

1.2 Objectives

The objectives of the present program are to develop improved sintering procedures to produce inertial-grade $SmCo_5$ magnets with improvements in the following areas:

(1) Long-term flux stability at constant temperature (140°F)

Desired: 0.008 ppm/90-day

Present capability: Sintered: ~1 ppm/day
Plasma Sprayed: 0.05 ppm/day

(2) Thermal stability of residual induction

Desired: 0.1 ppm/°F

Present capability: 300 ppm/°F

(3) Tailoring of thermal expansion coefficient

Desired, same as beryllium: 6.8 μin./in.°F

Isotropic: 5.6 μin./in.°F

Oriented:

(a) Along magnetization direction: 2.8 μin./in.°F

(b) Normal to magnetization direction: 7.2 μin./in.°F

SECTION 2

MATERIALS AND PROCESS STUDIES

2.1 Previous Work

An interim report on the status of the program was submitted in July 1978 covering the progress up to the time.[1]* The abstract of that report is as follows:

> For inertial applications, aligned $SmCo_5$ magnets with high flux stability, close-to-zero reversible temperature coefficient of magnetization, and a thermal expansion similar to that of beryllium are required. High flux stability is being attempted by producing high H_{ci} (high resistance to demagnetization) and high H_k (high second-quadrant loop squareness) magnets through the attainment of fine grain size, low oxygen content, and high density in the material. Low reversible temperature coefficient will be achieved by suitable samarium replacement with a heavier rare-earth element, while the thermal expansion coefficient will be tailored (to that of beryllium) by controlling the alignment of the crystals in the magnet.
>
> In line with these requirements, a magnet sintering facility capable of ultra-high vacuum operation (10^{-6} torr capability at 1100°C) has been fabricated for oxygen-free processing of these magnets. Techniques for producing powder with low oxygen contamination (from the environment) have also been

* Superscript numerals refer to similarly numbered references in the List of References.

developed for this purpose. The total amount of oxygen incorporated into the powder is found to be considerably less than what is obtained with conventional procedures.

This has resulted in remarkably high values of H_{ci} and H_k in sintered $SmCo_5$ magnets produced so far. The unprecedented value of 29 kOe has been measured for H_k in a few of these magnets as compared to 5 to 10 kOe found in most commercial magnets. The energy-product values of these magnets have been limited to about 13 mGOe because of poor alignment. Investigations currently in progress are expected to result in substantial improvements in the values of the energy product.

Pressure sintering (hot isostatic pressing) techniques have also been used for densification of powder compacts. Close-to-theoretical values of density have been obtained using this process. Properties of magnets formed with very coarse powder (using this technique) were found to be quite comparable to what is available with present technology. With the use of finer-sized powder, magnets with outstanding properties are expected in the near future.

2.2 Subsequent Studies

Although our initial sintered samples had very high H_{ci} (40 kOe) and H_k (as high as 29 kOe), the energy product of 13 mGOe was less than what we desired. At this stage, we decided that the energy product should be increased to over 15 mGOe, without degrading the other second-quadrant characteristics. This would amount to raising the residual induction (B_r) to a value of 7.75 kG or over, from about 7.3 kG we have been producing in the earlier magnets. This would involve increasing the alignment of the c-axis of alloy powder particles in the magnetization direction during compaction. From our past experience, it was known that we should have been able to achieve the desired alignment very easily with the alignment field of 20 kOe that we have been using

during compaction. Therefore, it was somewhat of a surprise that our magnets failed to align properly. As stated earlier,[1] there could be two possible reasons for this type of behavior. Perhaps the powder particles retained cold work stresses, since we were producing very fine powder particle size. In such a case the magnetic-easy c-axis changes to a cone along the c-axis. A second reason would be that the aligning field was applied when the powder was already packed to a degree, inside the die, trapping part of the powder in random orientation.

A number of magnet samples were compacted using the same 20 kOe aligning field and same pressure of 75 klb/in.^{2}. The pressed compacts at ejection from the die had the thickness of 0.180 in. (0.45 cm). The only parameter varied was the spacing between the plungers at which the magnetic field was first applied. From there on, the field was left on while the plungers were brought closer together until the final compaction. These compacts were then sintered at 1118°C for 1-1/2 hours and aged at 950°C for 4 hours, followed by quick cooling. The measured magnetic values are shown in Table 1.

Table 1. Plunger spacing versus remanence.

Dist. Between Plungers (cm)	Sintered Density (% Theoretical)	B_r (kG)	$(BH)_{max}$ (mGOe)
0.5	91.6	5.6	7
0.8	95.3	7.1	12
1.2	94.3	7.3	13
1.6	94.0	7.2	13
2.0	94.5	7.2	13
2.5	94.8	7.2	13

The sample pressed at 0.5 cm spacing obviously was more or less fully compacted when the field was applied and, therefore, remained quite isotropic as indicated by a low B_r of 5.6 kG. A B_r of 5.6 kG is about the level of remanence that can be expected from a randomly

oriented $SmCo_5$ magnet. The alignment improved when the field was applied at a larger spacing. The maximum was obtained at a spacing of 1.2 cm. None of the values of B_r, however, were high enough to produce any more than 13 mGOe of energy product. This was, therefore, not a very productive effort, and we decided to determine if the high energy product could be obtained by introducing less cold work in the alloy powder.

Accordingly, we reduced the time of final grinding from 25 minutes, which we were using until then, to 15, 10, and 5 minutes. Figure 1 shows the variation of particle size with grinding time as expected. The interesting features of these powders are the sharp fracture surfaces on shorter grinding cycles, whereas the longer grinding time shows more rounded particles, indicating abrasion type of size reduction which is liable to incorporate stresses in the particles. Compacts were aligned and pressed in the usual manner and sintered for 1-1/2 hours at 1118°C, aged at 900°C for another 1-1/2 hours, and then quick cooled. The compositions used for these experiments were 35.5, 36.0, and 36.5 percent Sm, and balance Co. The results are shown in Table 2.

Table 2. Effect of particle size on magnetic properties.

Time of Grinding (min)	Composition (% Sm)	Density (% Theoretical)	B_r (kG)	H_{ci} (kOe)	H_k (kOe)	$(BH)_{max}$ (mGOe)
10	35.5	92.9	7.8	42	24	15
15	35.5	94.2	7.7	40	23	15
10	36.0	92.7	7.7	47	15	14
15	36.0	95.2	7.7	44	14	15
10	36.5	91.7	7.3	49	18	13
15	36.5	95.0	7.5	41	15	14

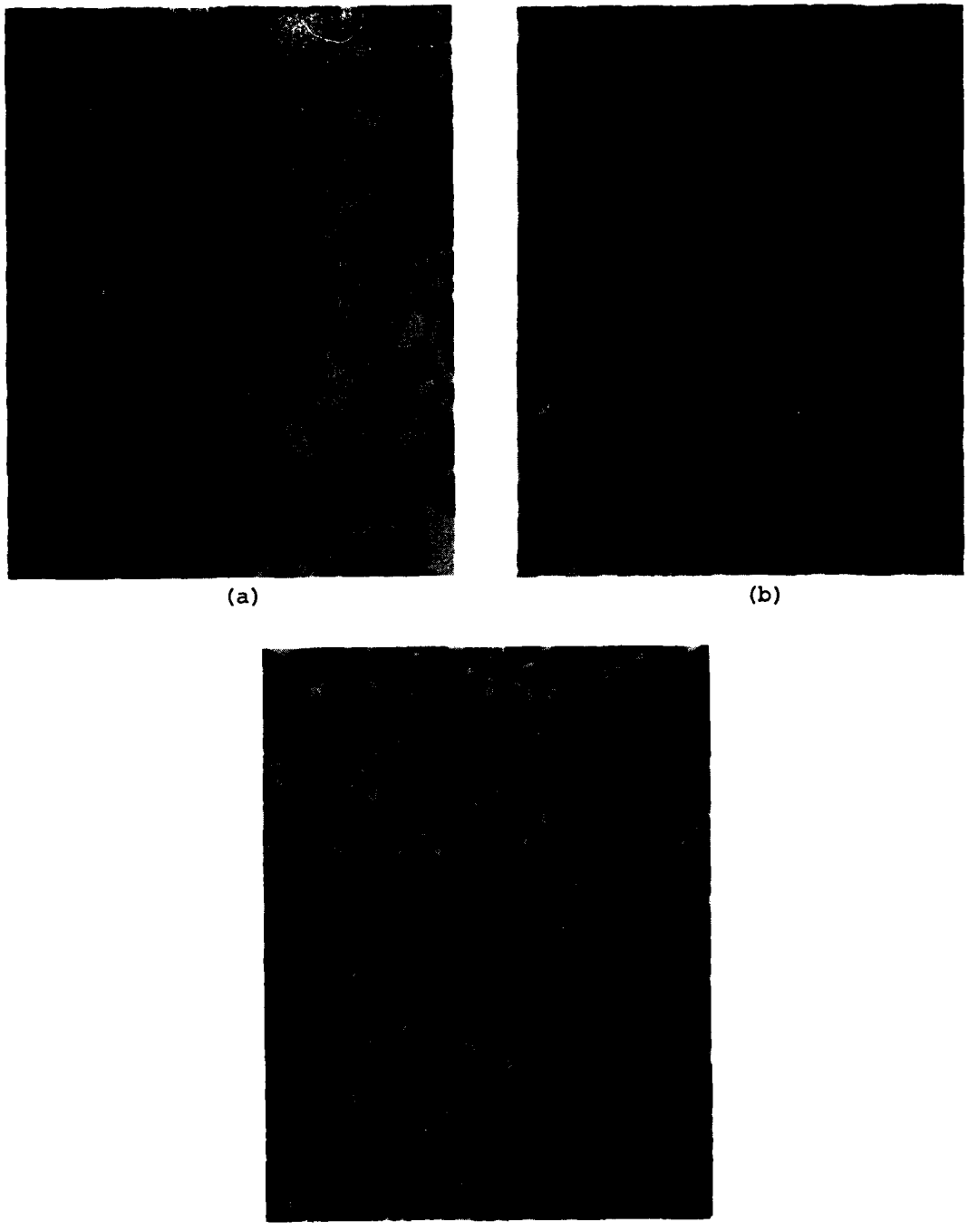

Figure 1. Particle sizes of $SmCo_5$ alloy due to different grinding time in attritor mill. (a) 5 minutes. (b) 15 minutes. (c) 25 minutes. Magnification approximately 400×.

Compacts pressed from 5-minute ground powder did not shrink to good density, indicating that higher temperature would be required for this powder. Measurements are therefore shown only for the 10 and 15 minute samples. Both 35.5 and 36.0 percent alloys at both the powder sizes gave the desired residual magnetization and energy product with quite high H_{ci} and H_k, and were, therefore, considered to be adequate.

However, it was desirable to have a still higher energy product to go with the high values of H_{ci} and H_k we had produced in these magnets. This would, of course, require further increase in magnetic alignment. There appeared to be two possible ways of accomplishing it. One of these was to superimpose a high level of pulsed field of the order of 50 kOe, of about 10-millisecond duration, repeated a number of times, on top of the 20 kOe dc field. The other choice was to cold isostatically press (CIP) the powder after aligning it in a 140 kOe dc field. In either case, the powder compacts would be sintered and aged in the conventional manner. We chose to CIP and sinter the 15-minute ground powder, and tried various composition ranges between 35.0 and 37.0 percent Sm content. Various sintering and annealing cycles were used. The best results were obtained with the 36.5-percent Sm powder sintered 3 hours at 1118°C and aged at 900°C for 17 hours, followed by quenching. The measured magnetic properties were:

B_r	8500 G
H_c	8400 Oe
H_k	28,500 Oe
H_{ci}	39,000 Oe
$(BH)_{max}$	18 mGOe

Unfortunately, about the time we had achieved the desired magnetic properties we had also exhausted the inventory of our initial alloys. Therefore, we acquired a new supply of 34.5 and 42 percent Sm alloys.

The new alloys showed a slightly different behavior, and we had to establish the optimum processing conditions again. The best results were obtained when the 34.5-percent alloy was ground for 20 minutes and the additive alloy (42 percent) was ground for 15 minutes prior to blending to obtain various compositions. Whereas the best results were obtained using 36-percent Sm composition with the older alloys, the new alloys required a blended composition of 36.5-percent Sm for die pressed and sintered magnets. Subsequent analysis of the oxygen content partly explains why the higher percentage of Sm was needed in the newer alloys. We have been able to maintain an average O_2 content of 0.3 percent in the blended old alloy powder, but the O_2 content had jumped to 0.6 percent in the new alloy blends, although we had followed identical procedures for powder preparation. It is not possible at this point to explain this different oxidation behavior, since it would perhaps require some very fundamental studies to be able to do so.

Using 36.5-percent Sm blend of the alloys, we studied the time/temperature variations of sintering and annealing cycles for both die-pressed and CIP'ed compacts as related to the intrinsic magnetic parameters. In Tables 3 and 4 the results of these studies are presented.

Table 3. Magnetic properties of 36.5-percent alloy blend die-pressed and sintered magnets.

Sample No.	Sinter-Anneal Cycle*	Density (% Theor.)	B_r (G)	H_c (Oe)	H_k (kOe)	H_{ci} (kOe)	$(BH)_{max}$ (mGOe)
21	1124°C - 3 h 900°C - 24 h	96.6	8350	8100	19.5	47	17
20	1118°C - 3 h 900°C - 24 h	96.3	8400	8300	17	46.5	17.5
23	1113°C - 3 h 900°C - 24 h	95.6	7800	7800	28.5	45.5	15
24	1108°C - 3 h 900°C - 24 h	94.0	7600	7600	33.5	44	14.5

* Following the 24-hour 900°C treatment, the samples were quick cooled by pulling the samples out to a water cooled section of the muffle.

Table 4. Magnetic properties of 36.5-percent Sm alloy CIP'ed and sintered magnets.

Sample No.	Sinter-Anneal Cycle*	Density (% Theor.)	B_r (G)	H_c (Oe)	H_k (kOe)	H_{ci} (kOe)	$(BH)_{max}$ (mGOe)
33	1110°C - 3 h 900°C - 24 h	94.0	8000	7950	24	33	16
35	1106°C - 24 h	94.4	8150	4450	2	6	9
35	Above sample further treated 1106°C - 1 h 900°C - 24 h	94.9	8350	8350	25	35	17
36	1106°C - 3 h 900°C - 24 h	91.5	7350	7300	26	37	13
38	1110°C - 3 h 900°C - 24 h	92.7	7500	7400	20	35	14
38	Further treated 1110°C - 24 h 900°C - 24 h	94.7	7700	7650	22	39	15
38	Further treated 1110°C - 24 h 900°C - 24 h	94.8	7750	7500	25	44.5	15

* All samples quick cooled following the thermal treatment.

Although the first two samples in Table 3 showed H_{ci}'s over 45 kOe and desirable energy products of over 17 mGOe, the second quadrant curves showed a definite depression in $4\pi M$ at comparatively low demagnetization field. This resulted in a lower H_k than the next two samples sintered at lower temperatures. The latter two magnets appear to be more desirable from the point of view of higher resistance to demagnetization (and perhaps also higher stability) although the energy products were somewhat lower. In fact, we picked the sample No. 24 for stability measurements. This has an H_k of 33.5 kOe which is, we believe, the highest ever recorded.

All the samples in Table 4 show fairly high values of coercivity related properties and acceptable B_r and $(BH)_{max}$, except the first run on No. 35. This sample was furnace cooled and resulted in poor properties. However, when it was rerun at sinter temperature for 1 hour followed by aging at 900°C for 24 hours and then quickly cooled, the expected high values were obtained. An interesting fact is that we did not see the improved B_r in CIP-sintered over the die pressed ones as we had seen earlier in the older alloys. The differences in these observations are not understood at this time.

In Figure 2 the microstructures of a few die-pressed magnets which have been sintered at different temperatures are shown. The largest grain size is seen in (a) (sample No. 21) and the smallest in (c) (sample No. 23) in accordance with the sintering temperatures. Although the grain size in (a) is very large compared to that of (b) (sample No. 20), their coercivities are very nearly the same. The grain size of (c) (sample No. 23) is much smaller than in either (a) or (b). The H_{ci}'s in all three cases are the same, but the H_k value is much higher in (c) than in (a) or (b). That is, the hysteresis curve of (c) tends to be more rectangular than either (a) or (b). The grain sizes in the three samples fail to explain the differences in these magnets; however, the visible defects appear to give some clue. With decreasing grain size there is a tendency towards fewer defects per grain. In addition,

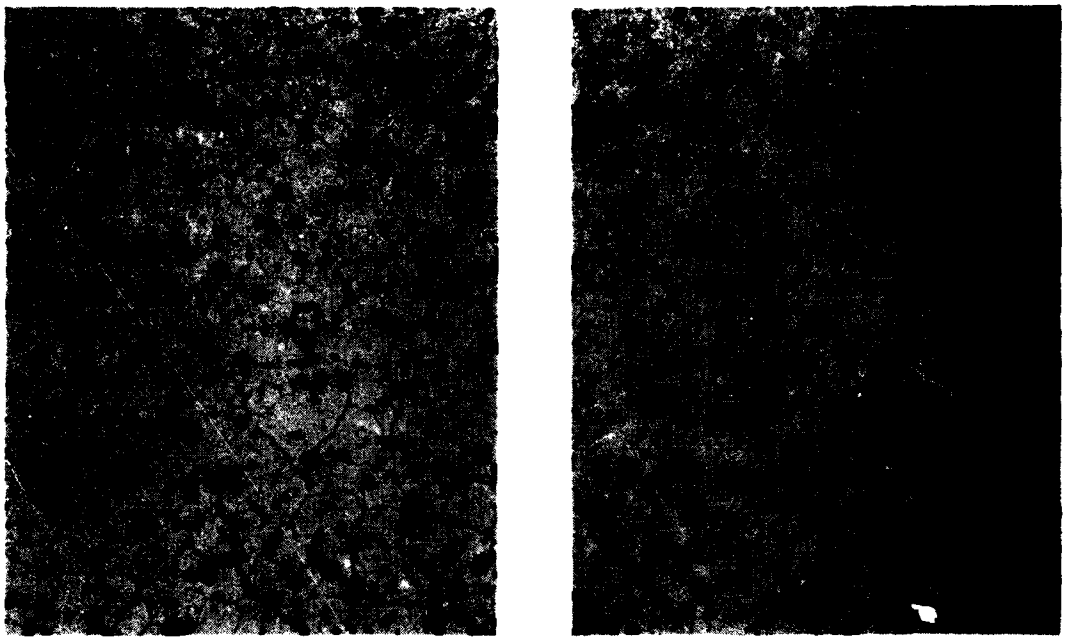

(a) (b)

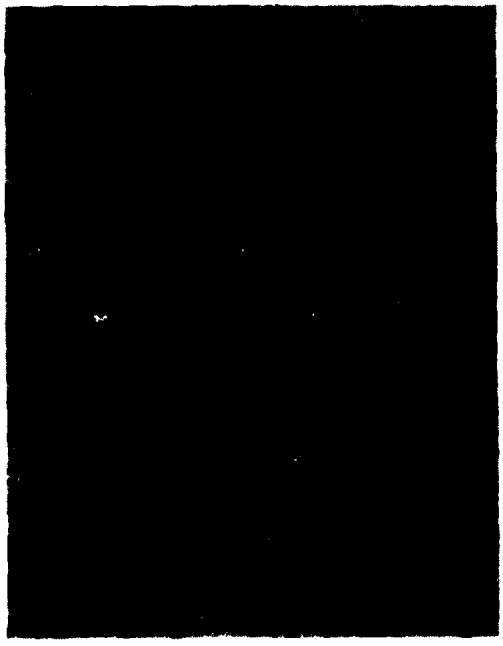

(c)

Figure 2. Microstructures of die-pressed sintered samples at approximately 400×. (a) Sample No. 21 sintered at 1124°C, (b) Sample No. 20 sintered at 1118°C, (c) Sample No. 23 sintered at 1113°C.

the defects appear to be along the grain boundaries when the grain size is small, while they appear to be within the large grains of microphotographs (a) and (b).

We had already seen that when the sintering temperature was higher than an optimum, there was a tendency for the demagnetization curves to show kinks. A kink is caused by the presence of two magnetic species; one with a higher coercivity than the other. Therefore, the effect of higher sintering temperature is the conversion of a portion of the material in the magnet to a lower coercivity magnet material. This could conceivably be due to a secondary grain growth phenomenon with the secondary large grains trapping a large number of defects, giving rise to domain nucleation within the grains instead of at grain boundaries. The effect of this would be to reduce the grain to a low coercivity particle. The microphotographs (a) and (b) of Figure 2 do seem to have some much larger grains than the bulk, and appear to have a large number of defects within these grains. In contrast, the grains in Figure 2(c) appear to be relatively free of trapped visible defects.

On the basis of the above reasoning, one could argue that, given enough time at a given temperature, the defects may migrate to the grain boundaries, especially if they had their origin in compositional inhomogeneity. We decided to carry on an experiment to see if such a possibility exists. A 36.5-percent Sm alloy magnet was first sintered at 1118°C for 3 hours with the normal subsequent aging and quenching. The magnet developed a very well-defined kink as shown in Figure 3(a). Subsequently three other thermal treatments were given to the sample, and magnetic measurements made after each treatment. The whole experiment and the results are shown in Table 5.

The kink in the demagnetization curve began to diminish following each of the thermal cyclings. The indication of that behavior is surmised from the gradual increase of H_k. In Figure 3, the four curves of the sample measured after each thermal treatment are shown.

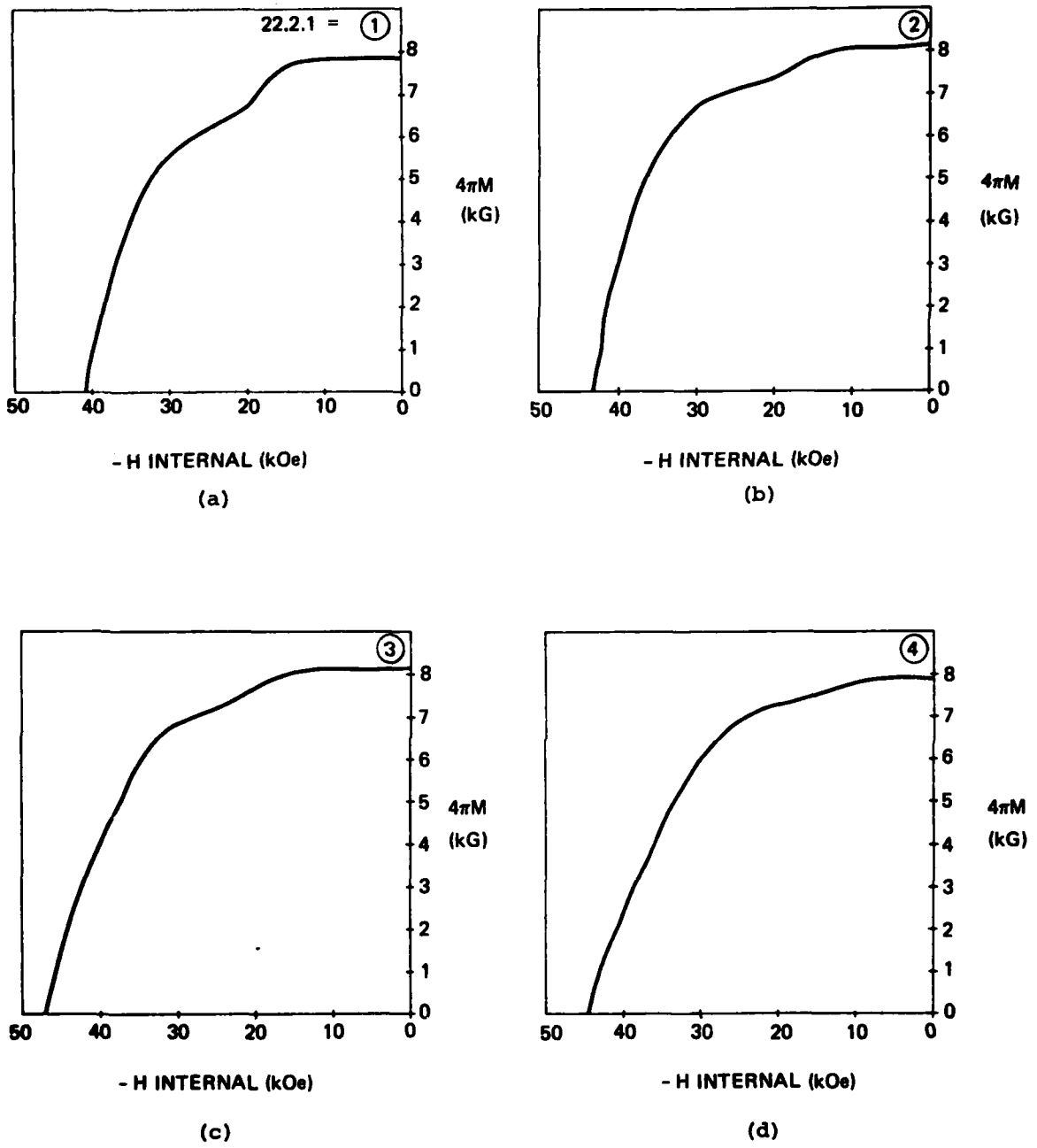

Figure 3. Demagnetization curves of Sample 22 (36.5-percent Sm alloy) after successive thermal treatments. Each of the high temperature treatments was followed by 900°C aging and quick cooling. (a) 1118°C - 3 h, (b) 1113°C - 3 h, (c) 1108°C - 3 h, (d) 1108°C - 3 h.

Table 5. Magnetic properties after repeated heat treatment.

Sample No.	Thermal Treatment	Density (% Theor.)	B_r(G)	H_c(Oe)	H_k(kOe)	H_{ci}(kOe)	$(BH)_{max}$(mGOe)
22	1118°C - 3 h 900°C - 24 h QC*	96.2	7800	7750	18	41	15
22	Additional 1113°C - 3 h 900°C - 24 h QC	96.2	8000	7950	20.5	42.5	16
22	1108°C - 3 h 900°C - 24 h QC	96.5	8050	8000	23.5	46.5	16
22	1108°C - 3 h 900°C - 24 h QC	96.5	7950	7850	24	43	16

* QC stands for quick cooling following annealing.

Various thermal aging experiments were carried out to see what their effects might be on the intrinsic magnetic parameters, in view of the fact that we had substantially improved the H_{ci} and H_k in these magnets over what is commercially available. Sintered magnets are known to suffer severe damage in the temperature range of 700 to 800°C. It was proposed by some researchers[2,3] that the degradation in this temperature range is caused by an eutectoid decomposition of $SmCo_5$ into Sm_2Co_7 and Sm_2Co_{17}. Using evidence gathered from Arc Plasma Sprayed magnets[5,6,7] we have clearly demonstrated that $SmCo_5$ is quite stable at all temperatures. However, Sm_2Co_{17} does form at lower temperatures from $SmCo_5$ by two distinctly different mechanisms. First, $SmCo_5$ can dissolve a certain amount of cobalt in excess of its stoichiometry which decreases with decreasing temperature. Therefore, depending on the alloy composition used, there can be a precipitation of the Sm_2Co_{17} phase in the cooling cycle. The second reason is the role oxygen plays in the precipitation. $SmCo_5$ at sintering temperature can dissolve oxygen in the range one percent or more (the exact value is not known) by weight. However, the solubility decreases as the temperature is lowered. The excess oxygen precipitates in the form of Sm_2O_3. The resulting depletion of Sm causes some Sm_2Co_{17} to form within or without the $SmCo_5$ grain. Regardless of the method by which Sm_2Co_{17} forms, it has a devastating effect on the magnet's ability to resist demagnetization.

Magnets were prepared with the compositions 36.0 percent Sm, 36.25 percent Sm, and 36.5 percent Sm by blending powders of alloys containing 34.5 and 42 percent Sm. Three samples of each composition were sintered at 1110°C followed by aging at 900°C for 24 hours, and then quick cooled. One sample of each composition was then reheated to 1110°C for 1 hour, aged at 900°C for 24 hours, and furnace cooled. The third set of samples was given a heat treatment of 700°C for 24 hours followed by furnace cooling. Magnetic measurements were made on each sample after each of the three thermal cyclings, and the data is shown in Table 6.

Table 6. Coercivity as a function of various thermal treatments.

Sample No.	Composition (% Sm)	First Heat Treatment 1110°C - 3 h, 900°C - 24 h Quenched		Second Heat Treatment 1110°C - 1 h, 900°C - 24 h Slow Cooled		Third Heat Treatment 700°C - 24 h Slow Cooled	
		H_{ci} (kOe)	H_k (kOe)	H_{ci} (kOe)	H_k (kOe)	H_{ci} (kOe)	H_k (kOe)
29	36.0	35	21	2	<1	0	0
30	36.25	36	24	9	4.5	0	0
31	36.5	42	29	23	19	6.5	3

The data indicated that the magnet with higher Sm content had higher resistance to temperature degradation, which confirmed previous observations.[4] We then decided to give a further long time treatment of 700°C to the sample already treated at 700°C for 24 hours. To the three samples from Table 6 we added a fourth one with 37 percent Sm, and exposed them to 700°C for 120 hours. The sample No. 31 showed an H_{ci} of 1.5 kOe further down from 6.5 kOe. The 37-percent Sm sample went down to 2 kOe. But the noteworthy fact is that samples No. 29 and 30, which had shown zero coercivity after 700°C for 24 hours, showed a positive value of coercivity around 500 Oe after an additional 120 hours at 700°C.

Since the 700°C treatment proved to be an undesirable treatment for these sintered magnets, a somewhat lower temperature (480°C) was selected, which could conceivably be used for relieving the thermal stresses caused by quenching from 900°C treatment. Accordingly, we picked a CIP-sintered and a die-pressed sintered magnet with excellent coercivities and gave them a thermal treatment of 480°C for 3 hours, followed by furnace cooling. Magnetic measurements showed that there was practically no degradation of properties, except for the H_k values which declined by 10 to 20 percent. The results are shown in Table 7.

Table 7. Magnetic properties before and after 480°C thermal treatment.

Sample No.	Thermal History	B_r (G)	H_c (Oe)	H_k (kOe)	H_{ci} (kOe)	$(BH)_{max}$ (mGOe)
33 (CIP)	As sintered at 1110°C and after 900°C	8000	7950	24	33	16
33	Additional 480°C 3 hours, slow cooled	8050	7850	20	31	16
40 (Die Pressed)	As sintered and aged	7800	7700	24	40	15
40	Additional 480°C 3 hours, slow cooled	7800	7700	22	40	15

SECTION 3

SPECIAL PROCESS INVESTIGATIONS

3.1 Hot Isostatic Pressing

The initial HIPing was performed on a coarse powder, a product of the double disc pulverizer. The best results were obtained on -400 mesh fraction which was given a 1000°C treatment and aged at 900°C after the HIPing. They were as follows:

B_r	8.1 kG
H_{ci}	27 kOe
H_k	16 kOe
$(BH)_{max}$	16 mGOe

For the as-HIPed condition, these values were 7.9, 4.0, 1.5, and 6, respectively.

Since the initial experiments in this area looked encouraging, we have gone further into this area. We had to resolve two issues if HIPing were to become a feasible method for fabricating magnets with superior properties. The first of these was the severe cracking of the samples either because of the thermal expansion mismatch between the sample and the stainless steel container, or because of the severity of the machining operation to remove the sample from the container. The other issue was the powder particle size. With large particle size we had produced reasonably good magnetic properties. Therefore, if we processed fine powder, the results would be superior magnetic properties.

In our next HIPing experiment we tried fine powder used for the sintering process and replaced the stainless steel container with copper. Copper proved to be an undesirable choice as it formed a low temperature melting alloy with Sm. We repeated that experiment using a low-carbon steel container with 1/8-in. wall thickness. This again resulted in severely cracked samples. In addition, the walls of the container reacted with the SmCo alloy, making it difficult to remove it.

We have resolved all of the above problems in our latest HIP experiment by adopting the following procedure. The container material was still a low carbon steel, but we reduced the wall thickness to ~ 0.030 in. from the 1/8-in. wall thickness we used before. In order to prevent the alloying reaction between the container wall and the SmCo alloy, we introduced a barrier layer of tantalum in the form of a thin foil wrapped around the SmCo compact. The removal of the steel container after the HIPing was easily accomplished by dissolving it in warm dilute nitric acid. The action of the acid stopped on reaching the Ta foil. The foil could then be peeled off quite easily, as shown in Figure 4. It was also quite gratifying to discover that the HIPed samples this time were free of cracks. Four samples with compositions varying from 35.5 to 37 percent Sm were included in this group. The powder used was coarse compared to sintering, i.e., the 34.5-percent alloy was attritor ground for 10 minutes and the 42-percent alloy ground for 7.5 minutes, compared to the 20-minute grinding time for sinter powder. Since no appreciable grain growth is expected to occur during densification, we should still expect good second quadrant properties. In addition, the larger particle size used resulted in a lower oxygen content. Detailed studies of these magnets are now in progress. Initial measurements in the as-HIPed condition are given in Table 8. Figure 5 shows the microstructures of the samples in the as-HIPed condition. Average $SmCo_5$ particle size appears to be around 15 microns, with a few larger ones as large as 20 to 25 microns.

Figure 4. Microphotograph of HIPed SmCo sample, showing the tantalum foil being peeled off following the dissolution of the steel container by HNO_3. Magnification 1×.

Table 8. Properties of HIPed magnets.

Sample No.	Composition (% Sm)	Density (% Theor.)	Oxygen Content (%)	B_r (G)	H_c (Oe)	H_k (kOe)	H_{ci} (kOe)	$(BH)_{max}$ (mGOe)
H-26	35.5	98.9	0.298	9050	8500	9	16.5	19
H-27	36.0	98.9	0.193	8600	8100	8.5	18.5	18
H-28	36.5	99.5	0.328	8600	7550	7	18	16
H-29	37.0	99.8	0.202	8250	7350	7.5	19	15

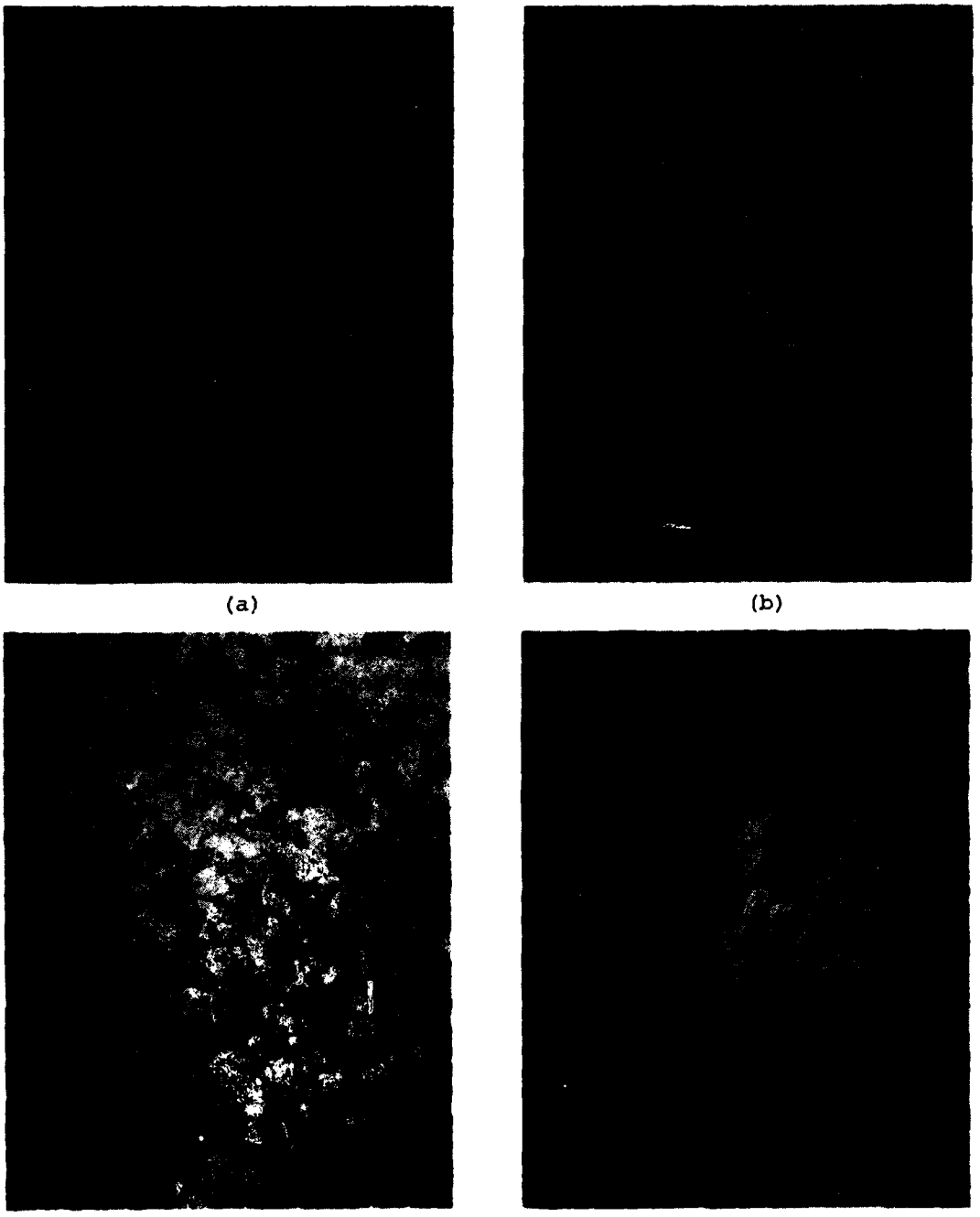

Figure 5. Approximately 400× microstructures of as-HIPed samples. (a) No. 26 - 35.5 percent Sm, (b) No. 27 - 36.0 percent Sm, (c) No. 28 - 36.5 percent Sm, (d) No. 29 - 37.0 percent Sm. Light grey phase is $SmCo_5$ and dark grey is Sm_2Co_7.

Second quadrant properties of this new batch of HIPed magnets are expected to reach similar values as our best sintered magnets after optimization of thermal treatments. However, since these magnets have lower oxygen content, it is possible they will have more stable performance and less degradation when exposed to intermediate temperatures. We will continue our studies to determine whether our assumptions are correct.

3.2 Stability Measurement

Since the H_{ci} and H_k values are the most important properties for highly stable performance, much of our efforts have gone into increasing these two properties in sintered $SmCo_5$ magnets. We have been remarkably successful in producing the highest H_{ci} and H_k values in sintered magnets that have ever been reported. Further improvements of these properties will not be easy to achieve without the expenditure of a great deal of effort and resources. The efforts should be directed towards substantially eliminating oxygen contamination along with further reduction of grain size.

The existing stability measurement device was described in the first report in July 1978, where we indicated that we would make some desirable modifications to make it more compatible with the necessary measurements in our magnet R&D programs. The concept is still in the design stages. In the meantime, our initial stability measurements have been made using the existing equipment. For this measurement, 12 identical rectangular magnets (approximately 0.1 in. × 0.12 in. × 0.25 in.), magnetized in a direction perpendicular to the 0.12 in. × 0.25 in. plane, were mounted on the outside wall of a well-annealed carpenter C-49 alloy hollow cylinder with an epoxy cement. The magnets were magnetized in a 140 kOe field prior to mounting, and they were mounted with the plane of magnetization on the cylinder wall, the longest edge parallel to the cylinder axis, and the adjacent magnets having opposite polarities. The multiple magnetic structure was then introduced into a permanent-magnet

torque generator circuit and rotated at constant speed over a period of time. The change in the output voltage in the generator coil, which is proportional to the magnetic flux, with time was then a measure of the decay of flux in the gap or the decay of magnetization of the magnet.

The magnet used in this first experiment was the No. 24 sinter run listed in Table 3. Enough magnets were sintered in this particular sinter run to fabricate two sets of samples for stability measurement. Each sample in this run was measured for magnetic properties and found to have no significant differences in properties. A set of representative values of the properties have been shown in Table 3. The first set of 12 magnets were magnetized, mounted on the C-49 ring using an epoxy cement, and cured at 150°C for 16 hours before being introduced in the torque generator circuit. The flux decay was then monitored and plotted on decay (in ppm) versus log time (in days) in Figure 6. When the time was measured from the time of magnetization the points fell on a straight line, with a slope of 762 ppm/decade. After this first measurement, the mounted magnet structure was given a thermal treatment of 225°C for 16 hours, following which we again monitored the flux decay rate for two decades of time. Initial plot of this data (shown in Figure 7), with the elapsed time being measured following the heat treatment, failed to fall in a straight line. To the time portion of this data we then added an additional 20 days. The result, shown in Figure 8, became a straight line once more with a slope of 700 ppm per decade.

The second set of samples of the sinter-run No. 24 have been given a 480°C - 3 hour aging followed by slow cooling to room temperature. Following the above treatment they have been magnetized and are now in the process of being mounted for stability measurement.

Besides the temperature stabilization treatments given so far, we expect to use oscillating magnetic field stabilization of these magnets to obtain more stable performance from these magnets.

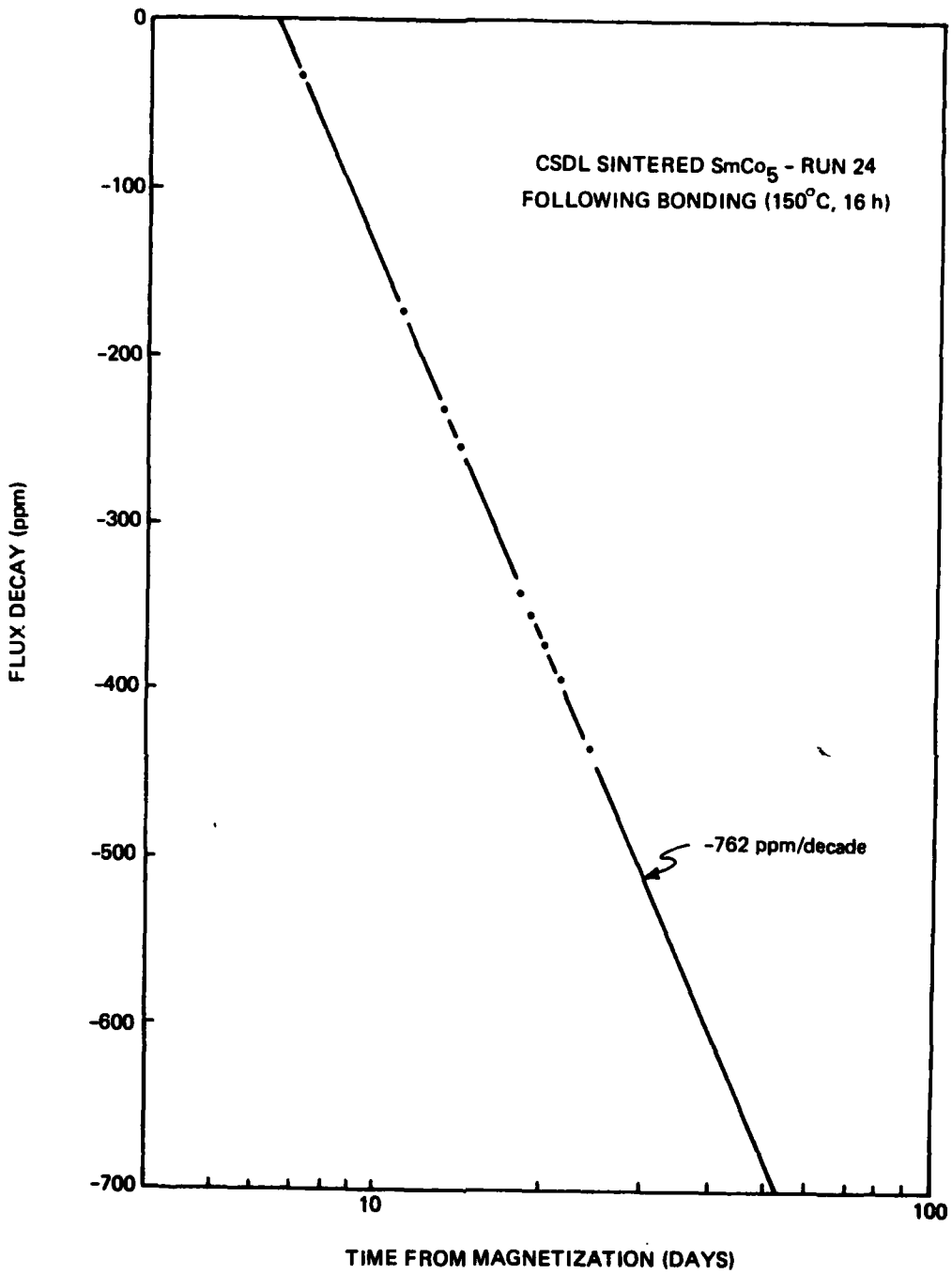

Figure 6. Flux decay plotted versus decade of days from time of magnetization.

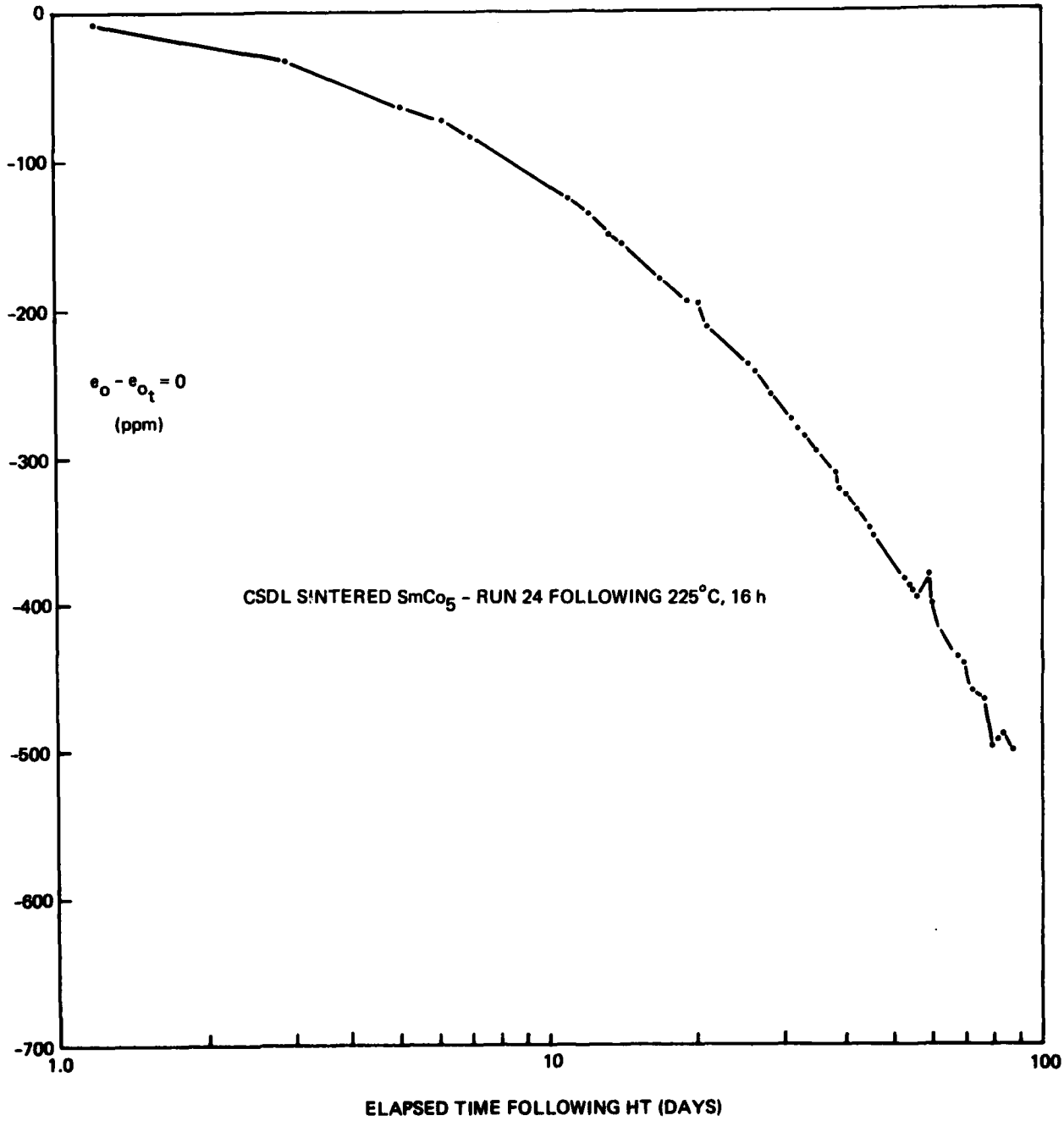

Figure 7. Flux decay curve of same set of samples as in Figure 6 after 225°C treatment. Time measured from the 225°C heat treatment.

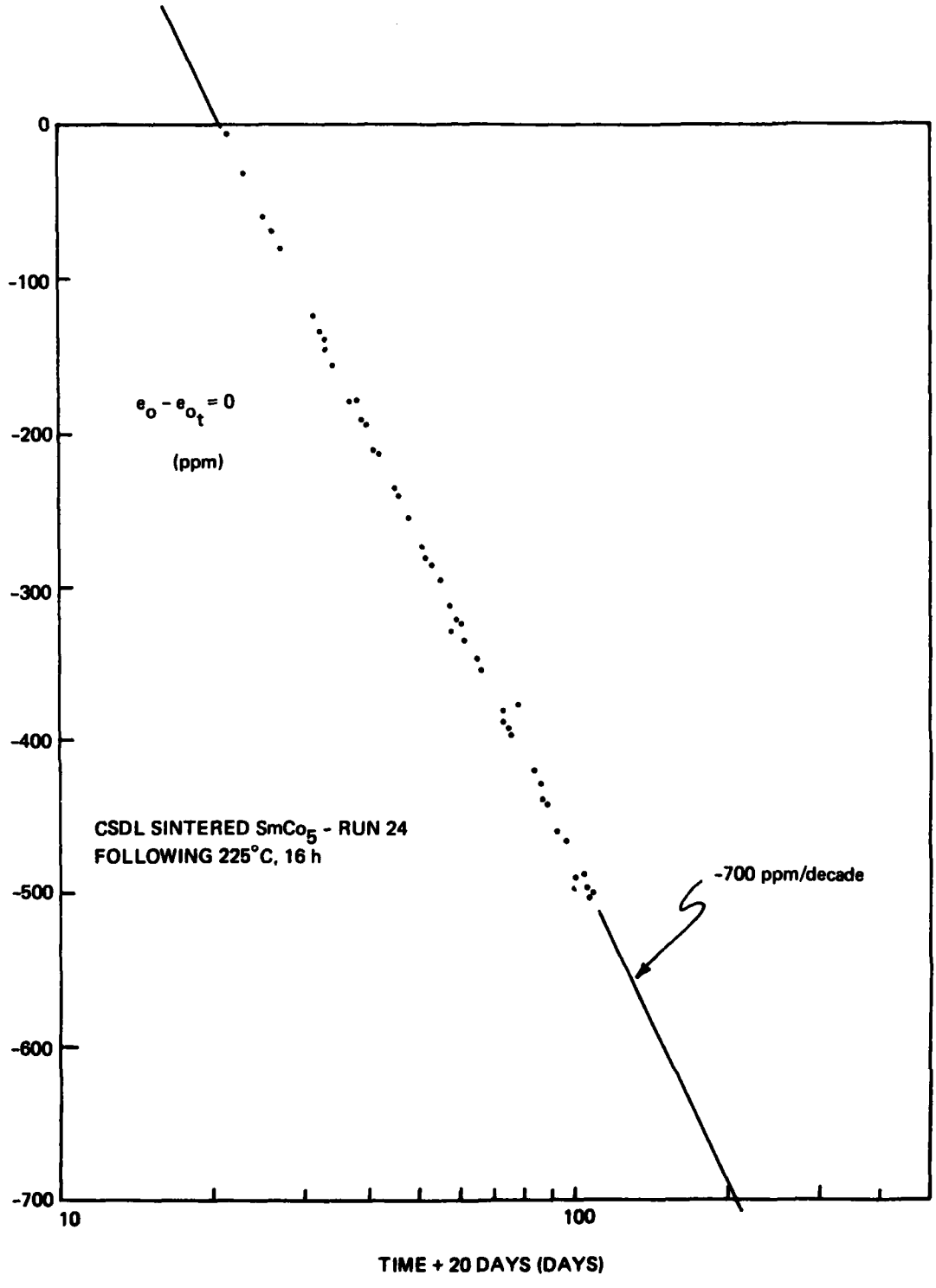

Figure 8. The decay data of Figure 7 replotted after addition of 20 days to the time of heat treatment. A reasonably good straight time plot is attained.

3.3 Chemical Comminution

We have been preparing the alloy powders by the conventional mechanical means, such as crushing, pulverizing, and grinding. During both the preparation and subsequent handling of the powder for the production of green compacts, the powder has to be more or less continuously exposed to air. It would, of course, be very desirable to avoid all exposure of the alloy to air from the time it is in the form of solid large pieces until the powder compact is fully densified. This would require a substantial investment in the form of a large controlled atmosphere chamber, where all the powder preparation machines are housed and all the necessary handlings are performed by means of mechanical manipulations. Acquiring such a facility is beyond the scope of this program. We are, therefore, looking at alternative means by which we could accomplish substantially improved results over present methods without large capital investments. This would involve chemical processes rather than mechanical means for comminution.

In 1969, Zijlstra and Westendorp[8] demonstrated absoption of very large quantities of hydrogen by $SmCo_5$ alloy under pressure at room temperature. The absorbed hydrogen is released when the pressure is reduced. The absorption resulted in the formation of complex hydrides of $SmCo_5$ alloy.[9] Work performed at G.E.[10] has shown repeated hydrogenation results in crumbling and disintegration of the alloy. Kuijpers[11] has since prepared 1-10 micron size powder out of $LaCo_5$ and $CeCo_5$ alloys by subjecting the solid pieces of alloys to a hydrogen pressure of 100 atmospheres for several hours. If we can produce $SmCo_5$ alloy powder by the hydrogenation process, with no exposure to air at all, the oxygen content of the powder will be no higher than in the alloy itself. The alloy that we purchase contains less than 0.1 percent oxygen, usually in the range of 0.05 percent by weight. But our sinter grade powder usually ends up with an oxygen content of around 0.6 percent. Using a fairly inexpensive inert-gas glove-box, we can take advantage of the chemically ground powder and CIP-HIP technique to achieve a densified $SmCo_5$ magnet with oxygen content of about the same percentage as in the starting alloy.

We have done some preliminary work in this area of hydrogen comminution. A small cylindrical stainless-steel can with a capacity of about 20 cm^3, and capable of withstanding several thousand $lb/in.^2$ pressure with an O-ring flanged enclosure, has been built. Stainless-steel tubings with high pressure valves and connectors were used for attaching the pressure can to a hydrogen tank (the source of hydrogen pressure), a vacuum pump, and an argon source. The first run of comminution involved a few 1/2-in. size alloy pieces passed through four cycles of pressuring at 700 $lb/in.^2$ of hydrogen and examination. Figure 9(a) is an SEM picture of the resulting powder, with particle size as large as about 100 microns. Some of the particles looked quite cracked, indicating that they would crumble to much finer size with a small mechanical force. This powder was then spatulated on a steel plate and sieved through a 400-mesh screen. Approximately 50 percent of the powder went through. Figure 9(b) is that of the -400-mesh fraction, which shows that there are many particles in the 1-10 micron range. Since the initial experiment, we have modified our equipment to be able to withstand up to 2000-$lb/in.^2$ pressure. At this moment, it looks promising that we may be able to produce sinter grade powder by this technique. We expect to continue further studies in this area.

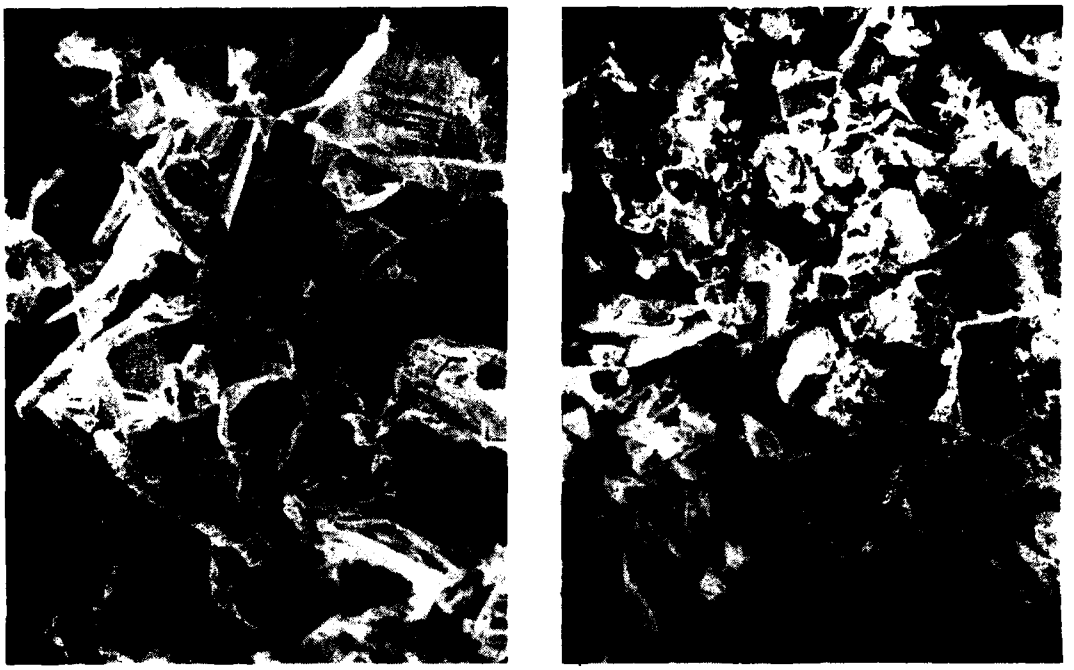

(a) (b)

Figure 9. SEM photographs of the hydrogen-comminution powder of $SmCo_5$ alloy. (a) as processed using 4 cycles of hydrogen pressurization at 700 lb/in.^{2}, (b) -400 mesh after spatulation of powder in (a) and sieving through 400-mesh screen. Both the photographs were taken at 500× magnification.

SECTION 4

DISCUSSION AND CONCLUSIONS

The decay rate of flux in our sintered $SmCo_5$ magnet with an H_k of 33 kOe, held at a temperature of 65°C, was determined to be around 700 ppm/decade of days. Similar measurements on our plasma sprayed magnets yielded a decay rate of about 50 ppm/decade.[12] The best available commercial magnets with H_k around 16 kOe under similar conditions of measurements showed a decay rate of 900 ppm/decade. The above findings contradict the reported H_k dependence of flux stability.[13] The best commercial sintered magnets contain a little higher amounts of oxygen than our sintered magnets, and the oxygen content of our Arc Plasma sprayed magnets is much smaller. Some plausible explanations of the measured decay characteristics can be given on the basis of oxygen content as discussed below.

According to Bartlett and Jorgensen[14] oxygen is soluble in $SmCo_5$, and the solubility increases with temperature. In fact, they claimed that $SmCo_5$ dissolves about 0.35 percent more oxygen at 1120°C (sintering temperature) than it does at 800°C. The amount dissolved at 800°C is not known. Our own conclusion at this time is that the oxygen solubility at 900°C is less than 0.6 wt percent (found in our sintered magnets), but more than 0.2 wt percent contained in our plasma sprayed magnets. Bartlett and Jorgensen also suggested that, when the temperature of the $SmCo_5$ is lowered so that the oxygen may precipitate out of solution, it does so by the formation of Sm_2O_3, with a resultant depletion of Sm in the surrounding site of Sm_2O_3 precipitation. The depleted

zone could conceivably form Sm_2Co_{17}, which requires less Sm than does $SmCo_5$. These then would be the defect sites where reverse magnetic domains would nucleate, which would result in a lowering of coercivity.

If there is an excess Sm present in the magnet body, and the temperature at which oxygen precipitation occurs is sufficiently high so that there is rapid enough diffusivity of Sm, then the depleted regions could be reconverted to $SmCo_5$ and the coercivity restored, or even improved, because of lesser amounts of oxygen dissolved in the $SmCo_5$ lattice. That, we believe, is the reason why sintered magnet coercivity is greatly enhanced when it is aged in the temperature range of 850 to 900°C followed by quenching. If, however, the precipitation of oxygen occurs in the temperature range of 650 to 800°C, the formation of Sm_2O_3 and Sm_2Co_{17} proceeds quite easily, but the kinetics of Sm diffusion is obviously much too slow to overcome the effect of damaging defects, and the coercivity drops drastically. Further down the temperature range, say 500°C or lower, the damage to coercivity is quite small, presumably because of a reduced kinetics of oxygen precipitation.

On the basis of the above explanations of the nature of oxygen reaction in $SmCo_5$, we can now examine the behaviors of both sintered and plasma sprayed magnets after different thermal treatments. The plasma sprayed magnet contains 0.2 percent oxygen, which appears to be completely soluble in $SmCo_5$ between 650°C and higher temperatures. We arrive at this conclusion from the fact that extended thermal treatments at any temperature from 650 to 1000°C of a well homogenized APS sample, followed by slow or fast cooling, have little effect on the high coercivities of these magnets.

As for our sintered magnets which contain 0.6 wt percent O_2, all of the oxygen appears to be in solution at the sintering temperature of around 1100°C. This concentration may not be the saturation limit, but it is higher than the solubility at 900°C, which we use as optimizing temperature. Indirect proof for the above statements is afforded by

the fact that the H_{ci} of this magnet, when it is cooled rapidly from 1100°C, is a lowly value of less than 10 kOe (see Table 4). This, we postulate, is the result of retaining all of a 0.6 wt percent O_2 in solid solution. If it is allowed to cool down to 900°C and held there for a period of time and then quenched, the coercivity H_{ci} can be as high as 45 to 50 kOe. This is the H_{ci} of the $SmCo_5$ material with the amount of oxygen it can retain in solution which is less than 0.6 wt percent at 900°C. The excess oxygen precipates out as Sm_2O_3. Sm_2Co_{17} formed during the precipitation of Sm_2O_3 is recoverted to $SmCo_5$ by the diffusion of Sm from the neighboring regions because of the excess Sm in sinter alloy. The holding time at 900°C is important in order to allow diffusion of Sm to proceed to completely eliminate Sm_2Co_{17}. The longer the holding time at 900°C, the higher the coercivity, up to a certain length of time beyond which there is no further improvement.

Let us now examine the absolute destruction of coercivity in the sintered magnets when subjected to extended heat treatments in the temperature range of 650 to 800°C. The explanation in this particular case is that the solubility of oxygen in the $SmCo_5$ is even lower now than at 900°C, and the process of Sm_2O_3 precipitation and the depletion of Sm in the surrounding regions continues. Of course, we still have excess Sm in the magnet body, but the neutralization of the depletion by diffusion does not happen readily, simply because the diffusion of Sm in $SmCo_5$ at these temperatures must be too low.

When the thermal treatment on sintered magnets is carried out at 500°C or lower after optimization, no significant deterioration was observed in the H_{ci} (see Table 7). A 10 to 20 percent decline in the H_k was seen in samples treated for 3 hours at 480°C, but the H_{ci}'s, H_c's, and B_r, etc. remained practically unchanged. The oxygen precipitation, although very slow, must still be there as indicated by the decrease in H_k values.

If the oxygen precipitation has slowed down to such a small value at 480°C, it appears unlikely that there could be any observable precipitation at 65°C, the temperature at which flux decay rates were measured. It should, however, still be a finite rate of precipitation, small though it may be. The flux decay rate in plasma sprayed magnets was found to be 50 ppm/decade, and 700 ppm/decade for sintered magnets. If the logarithmic relation between flux decay and time continues, as it is reported to be a well accepted phenomenon,[15] the total decay of flux over 27 years or 10,000 days (4 decades in days) will be 0.02 percent and 0.28 percent for the plasma sprayed and sintered magnets, respectively. The small decrease of coercivity associated with such small changes in the residual induction is beyond our measurement capability. It is, however, interesting to note that precipitation of oxygen at a given temperature should follow a logarithmic relationship with time just as the decay rate is found to be. For any given temperature, the rate of oxygen precipitation should also depend on the degree of supersaturation. It has already been brought out that the sintered magnets, after optimization treatment, contain substantially more oxygen in solution in the $SmCo_5$ lattice than the plasma sprayed ones. Therefore, it appears that oxygen plays an important role in the flux stability of $SmCo_5$ magnets, and our efforts should be directed towards the reduction of this very damaging element. Our new approach to powder preparation by chemical comminution appears to be a step in the right direction.

LIST OF REFERENCES

(1) Das, D., E. Wettstein, and K. Kumar, Technical Report R-1177, CSDL, July, 1978. Submitted to ONR under contract N00014-77-C-0388.

(2) DenBroeder, F.J.A., and K.H.J. Buschow, J. Less Common Metals, 29, p. 65, 1972.

(3) Martin, D.L., and J.G. Smeggil, IEEE Trans. Magnetics, Mag-10, No. 3, p. 704, Sept. 1974.

(4) DenBroeder, F.J.A., J. Zijlstra, J. Appl. Phys., 47(6), p. 2688, 1976.

(5) Kumar, K., D. Das, and E. Wettstein, J. Appl. Phys., 49(3), p. 2052, 1978.

(6) Kumar, K., D. Das, and E. Wettstein, IEEE Trans. Magnetics, Mag-14, No. 5, p. 788, 1978.

(7) Kumar, K., D. Das, J. Appl. Phys., 50(4), p. 2940, 1979.

(8) Zijlstra, H., and F.F. Westendorp, Solid State Comm., 7, p. 857, 1969.

(9) VanVucht, J.H.N., F.A. Kuijpers, and H.C.A.M. Bruning, Philips Res. Report, 25, p. 133, 1970.

(10) Raichlen, J.S., R.H. Doremus, G.E. Report 70-C-336, Oct. 1970.

(11) Kuijpers, F.A., J. Less Common Metals, p. 27, 1972.

(12) Recent unpublished work at CSDL may be presented at the Intermag. Conf. in April in Boston, MA.

(13) Mildrum, H.F., and K.M.D. Wong, Proc. Second International Workshop on R-Co Perm. Magnets, p. 35, June 1976.

(14) Bartlett, R.W., and P.J. Jorgensen, J. Less Common Metals, 37, p. 21, 1974.

(15) Dietrich, H.E., IEEE Trans. Mag., Vol. Mag-6, No. 2, p. 272, 1970.

BASIC DISTRIBUTION LIST

Technical and Summary Reports April 1978

Organization	Copies
Defense Documentation Center Cameron Station Alexandria, VA 22314	12
Office of Naval Research Department of the Navy 800 N. Quincy Street Arlington, VA 22217	
ATTN: Code 471	1
Code 102	1
Code 470	1
Commanding Officer Office of Naval Research Branch Office Building 114, Section D 666 Summer Street Boston, MA 02210	1
Commanding Officer Office of Naval Research Branch Office 536 South Clark Street Chicago, IL 60605	1
Office of Naval Research San Francisco Area Office 760 Market Street, Room 447 San Francisco, CA 94102	1
Naval Research Laboratory Washington, DC 20375	
ATTN: Codes 6000	1
6100	1
6300	1
6400	1
2627	1
Naval Air Development Center Code 302 Warminster, PA 18964 ATTN: Mr. F. S. Williams	1
Naval Air Propulsion Test Center Trenton, NJ 08628 ATTN: Library	1
Naval Construction Batallion Civil Engineering Laboratory Port Hueneme, CA 93043 ATTN: Materials Division	1
Naval Electronics Laboratory San Diego, CA 92152 ATTN: Electron Materials Science Division	1
Naval Missile Center Materials Consultant Code 3312-1 Point Mugu, CA 92041	1
Commanding Officer Naval Surface Weapons Center White Oak Laboratory Silver Spring, MD 20910 ATTN: Library	1
David W. Taylor Naval Ship Research and Development Center Materials Department Annapolis, MD 21402	1
Naval Undersea Center San Diego, CA 92132 ATTN: Library	1
Naval Underwater System Center Newport, RI 02840 ATTN: Library	1
Naval Weapons Center China Lake, CA 93555 ATTN: Library	1
Naval Postgraduate School Monterey, CA 93940 ATTN: Mechanical Engineering Department	1

BASIC DISTRIBUTION LIST (Continued)

Organization	Copies
Naval Air Systems Command Washington, DC 20360 ATTN: Codes 52031 52032	1
Naval Sea System Command Washington, DC 20362 ATTN: Code 035	1
Naval Facilities Engineering Command Alexandria, VA 22331 ATTN: Code 03	1
Scientific Advisor Commandant of the Marine Corps Washington, DC 20380 ATTN: Code AX	1
Naval Ship Engineering Center Department of the Navy Washington, DC 20360 ATTN: Code 6101	1
Army Research Office P.O. Box 12211 Triangle Part, NC 27709 ATTN: Metallurgy and Ceramics Program	1
Army Materials and Mechanics Research Center Watertown, MA 02172 ATTN: Research Programs Office	1
Air Force Office of Scientific Research Bldg. 410 Bolling Air Force Base Washington, D.C 20332 ATTN: Chemical Science Directorate Electronics and Solid State Sciences Directorate	1 1
Air Force Materials Laboratory Wright-Patterson AFB Dayton, OH 45433	1

Organization	Copies
NASA Headquarters Washington, DC 20546 ATTN: Code RRM	1
NASA (216) 433-4000 Lewis Research Center 21000 Brookpark Road Cleveland, OH 44135 ATTN: Library	1
National Bureau of Standards Washington, DC 20234 ATTN: Metallurgy Division Inorganic Materials Division	1 1
Director Applied Physics Laboratory University of Washington 1013 Northeast Fortieth Street Seattle, WA 98105	1
Defense Metals and Ceramics Information Center Battelle Memorial Institute 505 King Avenue Columbus, OH 43201	1
Metals and Ceramics Division Oak Ridge National Laboratory P.O. Box X Oak Ridge, TN 37380	1
Los Alamos Scientific Laboratory P.O. Box 1663 Los Alamos, NM 87544 ATTN: Report Librarian	1
Argonne National Laboratory Metallurgy Division P.O. Box 229 Lemont, IL 60439	1
Brookhaven National Laboratory Technical Information Division Upton, Long Island New York 11973 ATTN: Research Library	1

BASIC DISTRIBUTION LIST (Continued)

Organization	Copies	Organization	Copies
Library Building 50, Room 134 Lawrence Radiation Laboratory Berkeley, CA	1	Office of Naval Research Branch Office 1030 East Green Street Pasadena, CA 91106	1

SUPPLEMENTARY DISTRIBUTION LIST

Technical and Summary Reports

Professor Albert E. Miller
University of Notre Dame
Box 8
Notre Dame, IN 46556

Professor Karl J. Strnat
University of Dayton
Magnetic Laboratory
Dayton, OH 45469

Dr. J. J. Becker
General Electric Research
and Development Center
P.O. Box 8
Schenectady, NY 12301

Professor W. E. Wallace
Department of Chemistry
University of Pitsburgh
Pittsburgh, PA 15213

Dr. Richard P. Allen
Battelle-Northwest
Richland, WA 99352

Dr. Howard T. Savage
Naval Surface Weapons Center
White Oak
Silver Spring, MD 20910

Mr. Harold Garrett
Air Force Materials Laboratory
LTE, Bldg. 16
Wright-Patterson Air Force Base
Dayton, OH 45433

Dr. L. D. Jennings
Army Materials and Mechanics
Research Center
Watertown, MA 02172

Dr. J. O. Dimmock, Director
Electronic and Solid State
Sciences Program (Code 427)
Office of Naval Research
Arlington, VA 22217

Assistant Chief for Technology
(Code 2000)
Office of Naval Research
Arlington, VA 22217

Strategic Systems Projects Office
Department of the Navy
Washington, D.C.

Professor G. S. Ansell
Rensselaer Polytechnic Institute
Dept. of Metallurgical Engineering
Troy, NY 12181

Dr. David L. Martin
General Electric Research
and Development Center
P.O. Box 8
Schenectady, NY 12301

Professor M. Cohen
Massachusetts Institute of
Technology
Department of Metallurgy
Cambridge, MA 02139

Professor J. W. Morris, Jr.
University of California
College of Engineering
Berkeley, CA 94720

Professor O. D. Sherby
Stanford University
Materials Sciences Division
Stanford, CA 94300

SUPPLEMENTARY DISTRIBUTION LIST (Continued)

Dr. E. A. Starke, Jr.
Georgia Institute of Technology
School of Chemical Engineering
Atlanta, GA 30332

Professor David Turnbull
Harvard University
Division of Engineering and
Applied Physics
Cambridge, MA 02139

Dr. D. P. H. Hasselman
Montana Energy and MHD Research
and Development Institute
P.O. Box 3809
Butte, MT 59701

Dr. L. Hench
University of Florida
Ceramics Division
Gainesville, FL 32601

Dr. J. Ritter
University of Massachusetts
Department of Mechanical
Engineering
Amherst, MA 01002

Professor J. B. Cohen
Northwestern University
Dept. of Material Sciences
Evanston, IL 60201

Director
Materials Sciences
Defense Advanced Research
Projects Agency
1400 Wilson Boulevard
Arlington, VA 22209

Professor H. Conrad
University of Kentucky
Materials Department
Lexington, KY 40506

Dr. A. G. Evans
Dept. of Material Sciences
and Engineering
University of California
Berkeley, CA 94720

Professor H. Herman
State University of New York
Material Sciences Division
Stony Brook, NY 11794

Professor J. P. Hirth
Ohio State University
Metallurgical Engineering
Columbus, OH 43210

Professor R. M. Latanision
Massachusetts Institute of
Technology
77 Massachusetts Avenue
Room E19-702
Cambridge, MA 02139

Dr. Jeff Perkins
Naval Postgraduate School
Monterey, CA 93940

Dr. R. P. Wei
Lehigh University
Institute for Fracture and
Solid Mechanics
Bethlehem, PA 18015

Professor G. Sines
University of California
at Los Angeles
Los Angeles, CA 90024

Professor H. G. F. Wilsdorf
University of Virginia
Department of Materials Science
Charlottesville, VA 22903

SUPPLEMENTARY DISTRIBUTION LIST (Continued)

Dr. F. Rothwarf (DELET-ES)
Dept. of the Army
HQ, U.S. Army Electronic Command
Fort Monmouth, NY 07703

Mr. K. K. Jin
Strategic Systems Division
Autonetics Group
3370 Miraloma Avenue
P.O. Box 4192
Anaheim, CA 92803

Mr. N. Horowitz
The Aerospace Corporation
2350 East El Segundo Boulevard
El Segundo, CA

Mr. Francis W. Wessbecher
Unit Head
Inertial Component Engineering
Singer Kearfott Division
150 Totowa Road
Wayne, NJ 07470

National Magnet Laboratory
Massachusetts Institute of Technology
145 Albany Street
Cambridge, MA 02139

ATT: Dr. Donald T. Stevenson (2)
Assistant Director

Dr. C. W. Chang
G.E. Valley Forge Space Center
P.O. Box 8555
Philadelphia, PA 19101